

PROCEEDINGS OF SPIE

[SPIDigitalLibrary.org/conference-proceedings-of-spie](https://spiedigitallibrary.org/conference-proceedings-of-spie)

UV LED based gas correlation spectrometer of aromatics for the standoff detection of industrials spills and emissions

François Babin, Pascal Dufour, Félix Cayer, Jean-François Gravel

François Babin, Pascal Dufour, Félix Cayer, Jean-François Y. Gravel, "UV LED based gas correlation spectrometer of aromatics for the standoff detection of industrials spills and emissions," Proc. SPIE 10215, Advanced Environmental, Chemical, and Biological Sensing Technologies XIV, 102150Q (3 May 2017); doi: 10.1117/12.2263038

SPIE.

Event: SPIE Commercial + Scientific Sensing and Imaging, 2017, Anaheim, California, United States

UV LED based gas correlation spectrometer of aromatics for the standoff detection of industrials spills and emissions

François Babin^{*a}, Pascal Dufour^a, Félix Cayer^a, Jean-François Y. Gravel^a

^aInstitut National d'Optique, 2740 Einstein Street, Québec, Qc, Canada, G1P 4S4

ABSTRACT

Although there is a well-developed commercial offering for the detection of gaseous emissions in natural gas infrastructures, the same does not exist in the transport or transformation of liquid petroleum products. In the case of aromatics, UV DOAS using lamps and retroreflectors are amongst the only choices, along with UV-DIAL. But these are limited in sensitivity and depend on long absorption paths or are very complex. There are also large airborne lidars for the detection of liquid hydrocarbon spills on water or land that rely on UV induced fluorescence (LIF). But there is a lack of simple techniques for the remote detection of vapor plumes or spills involving liquid petroleum products. There have been proposals for the use of UV enhanced Raman for the detection of vapor plumes, but these require large laser powers and detection optics for poor sensitivity. On the other hand, recent developments in UV LEDs allows for simple techniques in the detection of aromatics, benzene and toluene in particular. These are found in most liquid petroleum products. Using these new commercially available UV LEDs and a gas correlation spectrometer set-up, benzene vapor is measured using the electronic transition at 258.9 nm and at other deep UV wavelengths. It is shown that while there is significant fluorescence in liquid benzene, oxygen in air severely quenches the fluorescence of the vapor phase benzene, rendering fluorescence unusable for the standoff detection of the vapor phase. Various implementations of standoff benzene/toluene detection using UV LEDs and gas correlation are discussed, along with pros and cons of the technique.

Keywords: Benzene, absorption, open path, gas correlation, LED, ultraviolet

1. INTRODUCTION

Benzene and other aromatics are widely used substances. Benzene is used in chemical substances such as plastics, adhesives, coatings, dyes, detergents, pesticides, lubricants, rubbers and of course are found in petroleum products. Presence of benzene and BTEX substances in general, in and around factories utilizing these chemicals, and more specifically refinery, production, processing or terminal facilities is an environmental issue as well as a health issue. These aromatics are carcinogenic. There is a push toward better monitoring of BTEX in the air in general and benzene around petroleum refineries or transfer facilities in particular. There is for example the requirements of 40 CFR part 61, Subpart BB for benzene transfer operations of the National Emission Standards for Hazardous Air Pollutants (NESHAP). The USEPA recently proposed a new method for fence-line monitoring of benzene in benzene refinery operations (Methods 325 A and B, *Volatile Organic Compounds from Fugitive and Area Sources*) to enforce new standards for benzene. The new methods involve air sampling with passive sorbent tubes. These methods are very sensitive, but are not real time measurement techniques. The sampling periods are normally of 14 days. Analysis of the tubes add significantly to the time before results are available. Sensitivities on the order of 160 ppt ($\sim 0.5 \mu\text{g}/\text{m}^3$) are said to be possible with this technique using flame ionization detection or mass spectrometry detection. Such a technique gives an average over multiple days, normally 14 in this case. The new rule requires that the difference between the lowest concentration and the highest concentration for two consecutive measurements be less than 2.8 ppb. On the other hand, average benzene concentrations in the air in the US are on the order of 160 ppt.

In parallel to these highly sensitive techniques requiring substantial sample handling, real-time optical measurement techniques are being refined. In optical sensing there also are gas sampling approaches, but these can be real time sampling techniques. Air samples are filtered and fill and flow through multipass gas absorption cells. The effective absorption length can be several tens of meters for cells measuring a few tens of centimeters in length (a typical path length of 50 to 80 m for a cell length between 30 and 60 cm). Long absorption paths are required for sensitive measurements. These cells require an air pumping mechanism, with filters, not compatible with simple, low maintenance, 24/7 field operation, although there are open, free flow multipass cells. Advantages of gas cells, in some cases, lie in the fact that pressure and temperature can be controlled and lead more easily to well calibrated measurements and allow fluorescence measurements at low pressure when fluorescence is quenched in air at

*francois.babin@ino.ca; phone 1 418 657-7006; fax 1 418 657-7009; ino.ca

atmospheric pressure. Fluorescence is often much more sensitive than absorption measurements, although more difficult to calibrate. These cells are even less field friendly systems. And these are still point measurements. In fenceline monitoring, path averaged concentrations are preferred. When using point sampling, multiple sampling points and multiple point measurement devices must be used all along the fenceline. Optical remote sensing and optical open path techniques are preferred. A single emitter/receiver system is often sufficient with a large open path distance for high sensitivity. UV-DOAS (UltraViolet Differential Optical Absorption Spectroscopy) is the standard open path optical technique for detecting benzene and other aromatics in air. In this case there is an emitter at one end of an open atmospheric path and a receiver at the other end. The path can be folded on itself using a large corner cube type retroreflector. This is the monostatic version, where the emitter and receiver are collocated. Large aperture emission and reception optics is usually used, typically in the 100 to 200 mm diameter range. Thoma et al ¹ tested different versions of a commercial UV-DOAS instrument, one being optimized for fenceline monitoring of benzene. They concluded that the noise floor (3σ) for the fenceline optimized version was on the order of 0.1 ppbv of benzene for 323 m of path length (or 0.03 ppmv-m) for 5 minutes of measurement time and a synthetic dynamic background subtraction approach, not easily implemented in the field. Therefore, UV-DOAS can be very sensitive and would probably be adequate for fenceline monitoring of benzene concentration differences that must be less than 2.8 ppbv, and with a much better temporal resolution. Unfortunately, commercial UV-DOAS instruments are still too expensive for many applications. This paper attempts to propose a lower cost version of the UV-DOAS open path approach.

The cost of the UV-DOAS instrument depends on the optical source, the optical filtering and detection method and on the emitter and receiver optics. UV-DOAS instruments usually rely on an optical grating spectrograph and on a high power discharge lamp; xenon, xenon-mercury, deuterium or other discharge lamps. The spectrograph measures an optical spectrum with a limited optical resolution. In order to have a high optical resolution, the entrance slit of a grating spectrometer must be as small as possible, usually not in line with high power discharge lamps that emit in all directions. It also needs to be a fast optical spectrograph, in order to collect as much light as possible. For benzene, the best lamp solution seems to be the xenon flash lamp. The emitting surface is many millimeters in length by ~1 mm wide for these lamps. The typical total optical output of a small xenon flash lamp (for high UV spectral power density) consuming 5W of electrical power, between 230 and 280 nm, is on the order of 10 to 20 mW, or, on average, 0.2 to 0.4 mW/nm. But there is a line structure to the optical emission from the lamp. These flash lamps have a typical deep UV lifetime of 10^9 flashes and are typically used between 200 and 500 Hz, for a continuous lifetime of between 500 and 1200 hours, although there are lower power extended lifetime versions. High output usually means shorter lifetime. These lamps also require high voltage circuits, up to the kV level. The outputted optical spectrum will change with discharge voltage and time.

This paper presents work done on an open path gas correlation spectroscopy approach. The rationale is discussed, followed by the description of the experimental setup and results. A discussion of these results leads to pros and cons and limitations of the technique as presented. Alternate approaches are discussed.

2. RATIONAL

A lower cost light source that is also simple to implement is the UV light emitting diode (LED) ². There are now multiple suppliers of UV LEDs. The commercial offering of UV LEDs starts at ~240 nm. Laboratory versions have been made down to 220 nm ³. Deep UV LEDs have a full width at half maximum (FWHM) of approximately 12 nm. The optical spectrum of a typical 260 nm LED is shown in Figure 1. There are now 260 nm LEDs that output up to 6 mW of optical power at 100 mA of input current and at 5 to 7 V of driving voltage (0.5 to 0.7 W of electrical power). This is for an emitting surface of ~ 1 mm². This is more than 0.5 mW/nm of optical power at the peak wavelength. The peak wavelength can be changed by changing the LED temperature. It is not unimaginable to have a supplier manufacture a LED with an elongated rectangular surface for optimal coupling to a grating spectrograph slit. Another option, which also can work with discharge lamps, is to use fiber bundles that go from an irregular shape to an elongated rectangle for coupling to a spectrometer, but at an added cost and complexity. It is also possible to raise the emitting surface area, with power scaling linearly with surface area. And it is also possible to raise the driving current at the expense of lifetime. The lifetime (50% intensity drop) at 100 mA driving current is typically better than 3000 hours. And specifications are getting better rapidly. These deep UV diodes have the cost advantage of semiconductor batch processing.

If stabilization of the emitted optical spectrum is required, the LED needs to be temperature stabilized. This approach thus requires thermoelectric cooling (TEC) and temperature stabilization of the LED. If not required, the optical spectrum at the emission could be continuously measured, at the same time the return spectrum is measured, which is a

possibility when using an imaging grating spectrometer or an optical chopper (alternatively measuring the emitted or returned signal). There are not, as of yet, suppliers of deep UV LEDs packaged with integrated TEC elements. In the work presented here, the LEDs are mounted on large external TEC elements. So, minimally, xenon lamps can be replaced by deep UV LEDs. This leads to smaller, cheaper, less power hungry systems. Another advantage of LEDs is that they can be driven by low noise current sources and can be modulated up to more than 100 MHz.

In UV-DOAS the emitted and received optical spectra are measured and subtracted in order to get the extinction plus absorption spectrum. The extinction can be considered slowly varying when compared to the absorption spectrum and considered as an offset that can be eliminated. The greater the number of optical absorption lines used, the better the least square fit to the measured optical spectrum. Of course, this entails having a reference spectrum measured with the same instrument, having the same configuration, with the same measurement parameters and in similar temperature and pressure conditions. Usually, the spectra of the major interfering molecules are also required for optimal sensitivity. For molecular absorption lines that are spectrally narrow, the best sensitivity is obtained with a high optical resolution spectrometer. This is very seldom the case when using grating spectrometers, especially for field deployable UV-DOAS. Very high resolution grating spectrometers are large and heavy. Especially if coupling a maximum of light into the spectrometer is required.

There are multiple absorption lines in the solar blind UV for the aromatics of interest. Figure 1 presents the high resolution absorption spectrum of benzene. The data is from Fally ⁴. There are many absorption lines between 240 and 265 nm. A UV-DOAS open path instrument would use all or only one of the absorption lines. Ideally lines that do not show significant interference effects from other molecules, oxygen and ozone in particular. Superimposed is the normalized emission spectra of a 258 nm LED as measured with an Ocean Optics HR4000-UV-NIR with 5 μm slits. The light from the LED is directly coupled to the spectrometer entrance slit.

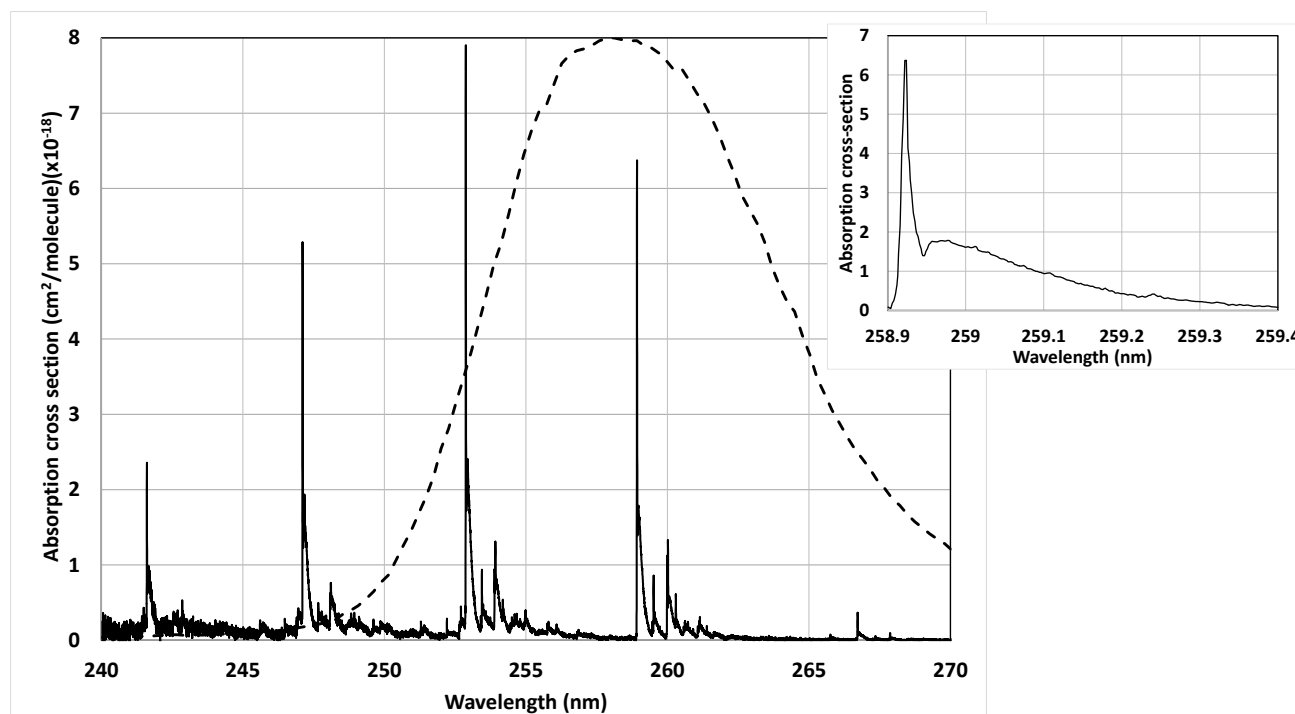


Figure 1. Absorption spectrum of benzene and emission spectrum of LED (in arbitrary units). Inset is expanded view of lines around 259 nm.

The absorption spectrum of Figure 1 is for benzene at low pressure (an average between 1 and 3 Torr) and at 293 K. The absorption spectrum is instrument limited (~ 7 pm). The absorption linewidth is unknown at atmospheric pressure in air, especially in light of the fluorescence quenching in the presence of oxygen (which significantly shortens the upper state lifetime). In any case, the absorption linewidth of the major peaks is expected to be less than 7 pm. The amount of photons from the unfiltered LED that can be absorbed is very limited for the major peaks. Absorption measurements with an instrument resolution on the order of 0.2 to 0.3 nm or more will rely on the contribution of multiple lines, as can

be seen from the deformation of the peak towards the longer wavelengths (inset of Figure 1). Using both the 252.9 and the 258.9 nm lines in the UV-DOAS fit would be ideal with the LED shown in the figure.

Other ways of measuring absorption have been devised. The one that is presented here is gas correlation absorption spectroscopy. This technique relies on the use of an absorption cell containing the molecule to be detected and acting as a tuned filter. The difference in absorption between gas cell filtered light and non-filtered light is a measure of the absorption by the molecule of interest. The gas correlation cell replaces the spectrometer of the UV-DOAS approach. This approach does not require a detector array as in the detection plane of a UV-DOAS spectrograph. The setup presented here is similar in nature to that presented by Kebabian et al ^{5,6}.

3. EXPERIMENTAL SETUP

The experimental setup is shown in Figure 2. Two deep UV LEDs from Nikkiso are mounted on TECs. Their peak wavelength is between 258 and 259 nm at 25°C. Their FWHM is 12 nm. They emit approximately 2 mW of power over 130° FWHM at 100 mA of drive current. The current drivers are Wavelength Electronics QCL low noise current drivers QCL1000+, with a current modulation input at 0.2 A/V. The LEDs are temperature controlled with Wavelength Electronics MPT10000 controllers. A first very high numerical aperture anti-reflection (AR) coated fused silica lens intercepts a large part of that light (Edmund Optics 67-270, 10.4 mm back focal length, 20 mm focal length, 22.5 mm clear aperture). A little less than 50% of the emitted light is collected. A second AR coated lens, immediately after the first, images the LED between 50 and 100 cm away (Edmund Optics 48-292, 400 mm focal length, 24 mm clear aperture). A first LED beam passes through a gas correlation cell (Reflex Analytical 5900SS, Stainless steel demountable cell, 10 cm long, 25 mm clear aperture) with AR coated fused silica windows (Thorlabs VPW42-UV). Upon exiting the cell the beam is folded with a 75 mm diameter UV enhanced aluminum mirror (Edmund 84-425) and routed to a 50/50 beam combiner/splitter (Thorlabs BDP508-FS). The beam combiner reflects this first beam toward a measurement cell. This measurement cell simulates an open optical path. It is similar to the gas correlation cell, except that it is connected to a vacuum pump and a gas handling system. A calibrated 100 ppm bottle of benzene in air is used to fill the measurement cell. The measurement cell can be filled at different pressures, as measured by a pressure gauge (Omega PX309-015AI with DPi32 process controller). The light from the second LED is collected with a similar pair of lenses and aimed at the beam combiner. The light from this LED goes through the beam combiner. Both beams are then merged. The beams then pass through an optional bandpass interference filter, placed at an angle (Semrock LL01-266-25, with the filter function shown in Figure 4, with a clear aperture of more than 22 mm when not angled). Along the beam path a fused silica wedge (Thorlabs BSF20-UV, 45 mm clear aperture) collects approximately 2% of the beams for power referencing. This sample beam is optically filtered (Semrock FF01-260/16-25 bandpass filter, 260 nm center wavelength, 20 nm FWHM, 22 mm clear aperture) and focused with a third AR coated fused silica lens (Edmund 48-284, 50 mm focal length, 24 mm clear aperture) onto a UV enhanced silicon photodetector (Edmund Optics 54-037, 6.7 mm diameter active area). The focused spot from the LEDs on the detector is slightly more than 1 mm by 1 mm. A camera is used to align the spots of both LEDs one over the other in the focal plane, at the detector position. The photodetector is coupled to a transimpedance amplifier (homemade, 300 kHz 3 dB bandwidth). The electrical signal is then routed to a digitizer for further processing (National Instruments NI 6124 or homemade digitizer board).

The light beams that pass through the measurement cell go through a similar optical setup to that of the sample beam (filter, lens and detector). Both detection arms are similar in all aspects, except for position. The signals go to a similar transimpedance amplifier and are routed to the same digitizer, although on a different channel. The pressure in the measurement cell is not monitored once it is filled at a given pressure. The only monitored state is the vacuum state, since it is continuously pumped in order to evacuate any benzene desorbing from the cell surfaces. This is important for assessing the stability of the baseline measurements (no benzene in the cell).

The gas correlation cell is filled with air at atmospheric pressure and benzene. Benzene is introduced with a graduated pipette in the form of a drop of pure liquid benzene and left to evaporate. The concentration of benzene is calculated knowing the liquid volume and supposing all of the droplet as evaporated inside the cell. Adsorption to the cell surfaces is not considered. Benzene concentration must be such that practically no light at the major peak passes the cell.

The gas correlation approach uses an approach in which only one LED is driven at any one time ^{5,6}. In the measurements presented here, there are three periods. In the first, no LED is emitting (except for light from the leakage current of the drivers). The measurement taken during this period is termed the “offset”. This offset combines the electronic offsets and the little light from the leakage current. In the second period, only the LED (LED 2) in the arm containing the gas

correlation cell is emitting. In the third period, only the light from the other LED (LED 1) is emitting. The signals for this modulation come from the NI 6124 that are inputted to the modulation inputs of the LED current drivers. A real-time software measures the signal from the power referencing detector and adjusts one of the LED drive currents to keep the signals in periods 2 and 3 equal (period 2 minus offset and period 3 minus offset). The modulation signal comes from a 16 bits, ± 10 V waveform generator.

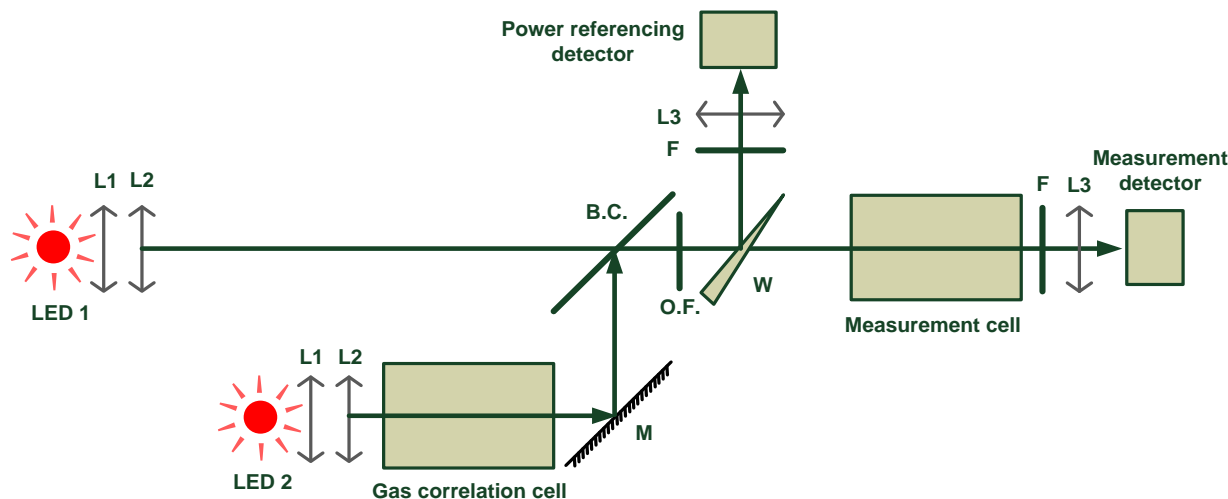


Figure 2. Experimental setup as described in text. L1, L2 and L3 are lenses. M is a mirror. B.C. is the beam combiner. O.F. is the optional filter. W is the wedge. F is the ambient light filter.

For the measurements presented here, each LED is driven for 3 ms, sequentially. An approximately equal offset time initiates a measurement period. Three plateaus are obtained during a period. There is then a dead time to transfer data to memory. The total period time is 25 ms. Only a third of the elapsed time is effective measurement time. This can be enhanced. From the digitized waveform, an average is made from the values of each plateau.

4. RESULTS

The signals on the measurement detector would ideally be equal when the measurement cell is empty. They are not. The difference in signal amplitude is different than that on the power referencing detector because the two bandpass filters that filter out ambient light are not exactly similar and the spectrum of light from the two emission arms are different (see Figure 3). Also, because of slight misalignments between the two arms and the fact that the optics, especially the measurement cell, clip part of the beams, there could be a differential clipping. Moreover, because of the angled components, there are polarization effects. It is thus normal not to have a zero offset even though the power referencing arm is kept close to zero difference. The goal is to measure as small as possible a difference between periods 2 and 3 on the measurement detector. Clearly, the major obstacle to measuring a very small concentration of benzene will be the stability of the baseline signal (the signal difference for which there is no benzene in the measurement cell). The filter functions along with the unfiltered LED spectrum are shown in Figure 4.

It would be possible to calibrate the power referencing arm to effectively have a zero difference in the measurement arm. It is not clear how this would affect the drift in the baseline (in the measurement zero in this case). It would also be possible to add an optical component after the power referencing wedge, in the measurement arm, to compensate for the difference (such as another appropriately angled wedge if the difference is found to be essentially due to polarization effects).

Figure 5 shows the results from correlation measurements in the measurement cell. First, the signal from the measurement detector in period 2 minus the offset on this detector divided by the same from the power referencing detector (period 2 minus offset) is computed (in order to compensate for noise from the LEDs). Secondly, the same is done for period 3. The correlation value is the difference between these two computed values. It was observed that part

of the “noise” on the measurement was in line with the temperature controllers, when the optional filter is not in place. If a step difference was made on the current driving one of the LEDs, the circuit was such that the other should follow. The temperature controllers then kick in to stabilize the temperature at the new drive currents. There are oscillations in temperature during this process. These oscillations are clearly seen on the correlation signal. This gives a clear indication on the impact of LED temperature on the stability of the baseline signal.

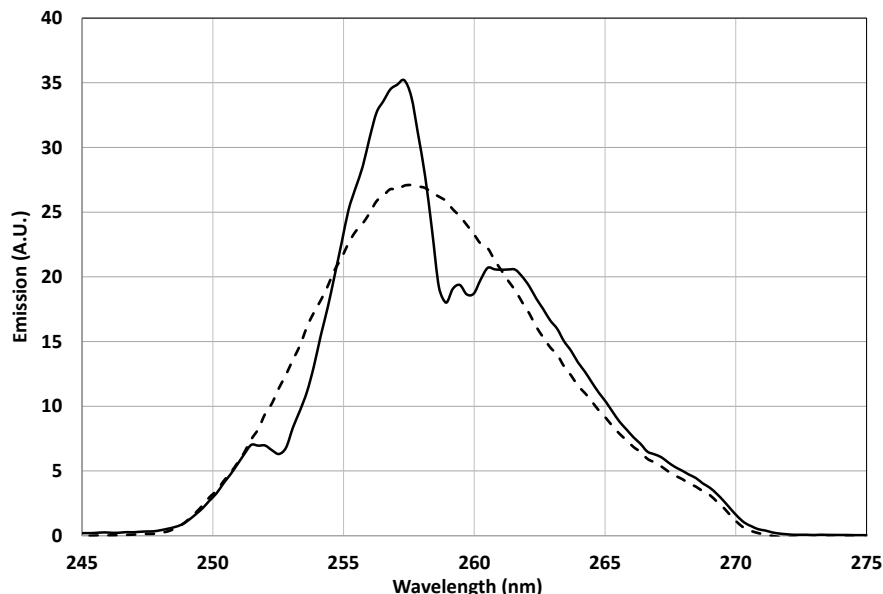


Figure 3. Spectra of the two LEDs at the measurement detector as measured through an optical fiber placed at the detector position.

Data from manufacturers of deep UV LEDs show that the LED maximum can shift by $0.03\text{nm}/^\circ\text{C}$ or more. Preliminary modeling using the manufacturer supplied filter function and the measured spectrum of a typical LED at 25°C shows a shift of 0.01°C between the temperatures of the two LEDs can mean a difference of almost 0.02% in the differential in filtered power. This temperature difference is more than likely to happen, being at the limit of the temperature controllers' specifications and the LEDs being mounted in open laboratory air on large TECs (these are not neatly packaged devices). It is expected that for this reason alone, the filtered power could vary by up to 0.05% or more. The interference filters also have a temperature coefficient, not specified by the manufacturer and not measured. The interference filters are not temperature stabilized and could potentially have temperature coefficients for the center wavelength of ± 0.001 to $\pm 0.01\text{ nm}/^\circ\text{C}$, probably in the lower range. A change of 1°C in the laboratory temperature could have a greater impact than a small difference in the temperatures of the LEDs. But again, it is the difference between the filtering for the two LEDs that is of importance. Moreover, as explained, the beams from the two separate arms can be slightly misaligned, both in optical axis and in divergence, especially if the LED is not stable in position because of temperature changes in the LED/TEC/heatsink holder. These parameters were not measured, the only precaution taken was to insure both images were on the small silicon photodetector at the alignment stage. This has an impact on the interference filter transmission function.

The absolute difference in signal amplitude between the empty measurement cell and a 10 ppm-m of benzene measurement cell, for the light beam not passing the gas correlation cell, is $\sim 0.4\%$. Thus, it could be expected that with this setup, baseline variations on the order of 1 to 5 ppm-m over tens of minutes could be observed. And this is the case. In order to limit this effect, another bandpass filter was used. This filter was inserted just after the beam combiner and filtered both beams. The filter's $\sim 2\text{ nm}$ FWHM limits the light to that which is close to the LED's spectral maximum, near 259 nm . There is then a single bandpass for both LEDs. No more differential filtering possible, except for slight angle changes between the incoming beams. Of course, with both filters (the optional filter and the ambient light filter in front of the detector), approximately 68% of the absorbed light at 259 nm is lost, other losses not considered. The

interference filter has a temperature dependence, but this shifts the transmission close to the LED's maximum, having much less impact on the baseline.

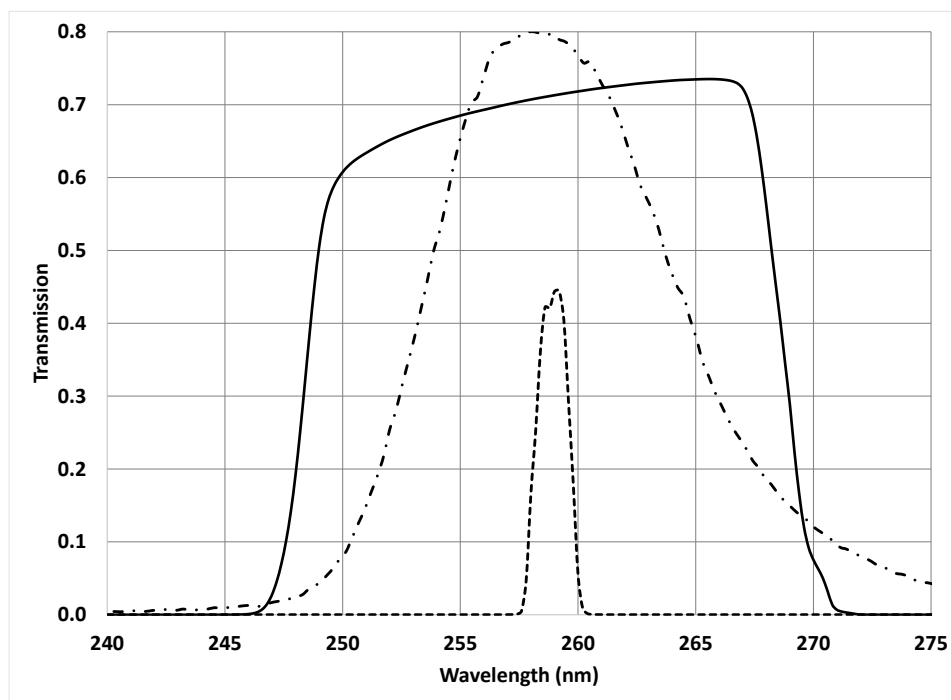


Figure 4. Filter function. Solid line: ambient light filter. Dashed line: optional bandpass filter. The dot-dashed line is the emission spectrum of a LED (in arbitrary units).

With the optional 2 nm FWHM bandpass filter in place, a series of measurements is done over a period of close to 40 minutes, as shown in Figure 5. The measurement sequence starts with a vacuum in the measurement cell. After each fill of the measurement cell and a small measurement period, there is a new vacuum period. So the sequence is vacuum, 10 ppm-m, vacuum, 5 ppm-m, vacuum, 2.5 ppm-m, vacuum, 1 ppm-m, vacuum. A first average of 100 consecutive 9 ms waveforms is performed, for 900 ms of effective measurement time (and 2.5 seconds of elapsed time). A correlation value is then computed. A rolling average is done over 60 of these correlation values for the data in figure 4. This translates to 54 seconds of effective averaging time. The time axis is the actual elapsed time for the measurements. The transitions are not shown. The steps are clearly visible between the different concentration values. No attempt was done at analyzing the noise on the different levels or at analyzing the linearity. The emphasis is on the baseline level and on the noise and drift of this baseline. This is what will ultimately limit the technique's sensitivity. There is a relatively strong dip in the baseline after the first 10 ppm-m step, and there seems to be a noticeable long term drift. A drift on the order of 0.2 to 0.3 ppm-m between the beginning and end of the sequence. The question arises as to why a dip after a relatively high concentration fill of the measurement cell. As will be discussed, benzene fluoresces significantly when oxygen is not present, and especially after filling a gas cell and subsequently emptying the cell, even if the benzene concentration is low. Desorbing benzene can fluoresce and add to the signal from the beam not going through the gas correlation cell. The measurement detector is rather close to the measurement cell. This would cause a dip in the baseline. It could seem a farfetched explanation, but one that merits investigation. This is not tackled in this paper.

These preliminary results show that it is possible to expect less than 0.3 ppm-m of long term drift. On a 300 m open path, this is equivalent to approximately 1 ppb. Which is still at least an order of magnitude too high when compared to fenceline benzene specific UV-DOAS.

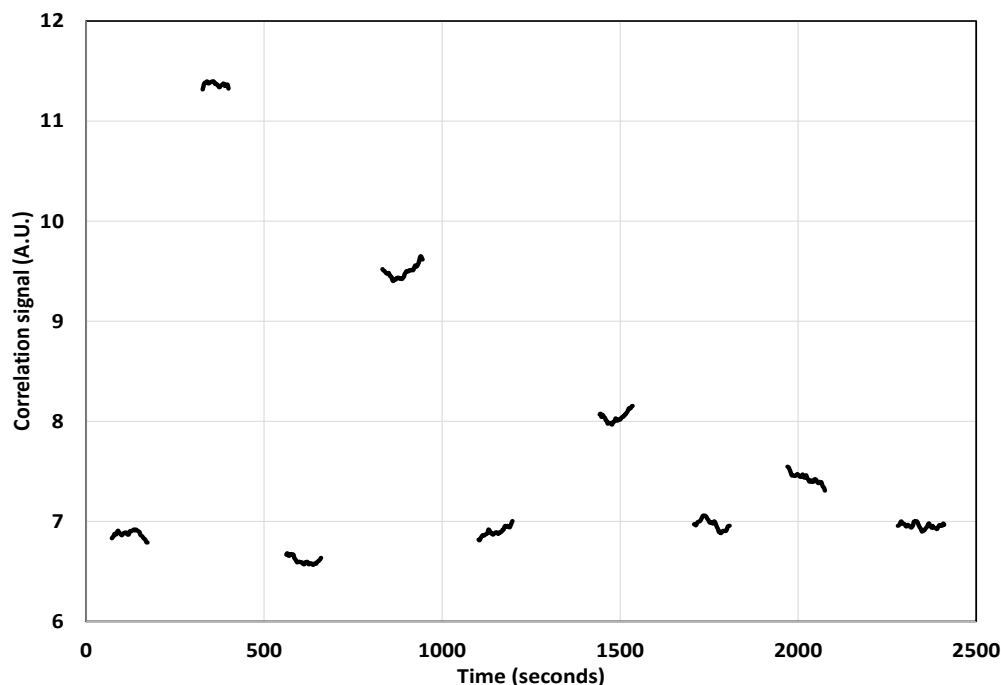


Figure 5. Results from a series of correlation measurements. The signals close to the 7 mark are empty measurement cells. The others are, respectively, 10 ppm-m, 5 ppm-m, 2.5 ppm-m and 1 ppm-m.

5. DISCUSSION

Besides the parameters that affect short, mid and long term stability of the baseline that were already discussed, there is also the question of the stability of the gas correlation cell. It is known that benzene photodissociates or photodegrades under deep UV illumination. What impact will this have on the long term stability of the baseline? The changes that are being measured when targeting sub-ppb levels are minute. This is another drawback of this technique. It works better on complex molecules when used in the infrared part of the spectrum.

In order to have better results, it would be wise to have a bandpass filter with a smaller FWHM. A bandpass of 0.3 to 0.4 nm would probably be ideal, although no simulations have been done. The baseline would be more stable. A double bandpass filter would be even better, using both 259 and 253 nm lines. It would also help if the effective emission spectrum had a flatter spectral distribution in the spectral region used for the measurement. This could be done with the interference filter (giving it an appropriate spectral transmission) or by adding multiple LEDs slightly shifted in peak emission (shifted by approximately the FWHM or ~6 nm). Slight temperature drifts would have less impact. These solutions add complexity. The goal is to have as little complexity as possible.

No attempt at determining the impact of interferents has been done. Since the absorption takes place over essentially 2 nm, this will be an issue⁷. Lowering the concentration in the gas correlation cell to be more specific could be required, but at the same time, the correlation signal will also be lowered. Multiple tries with different concentrations would allow optimization.

It is clearly not straightforward to design a low cost, low complexity, absorption based, open path gas correlation detector that has the same sensitivity as the reported optimized UV-DOAS approach. The question arises as to whether fluorescence would not be more sensitive. Fluorescence is in the solar blind region so that ambient light is not a problem if optically filtered. Strong fluorescence arises when on a molecular electronic transition, the same as for absorption. Fluorescence is thus measured with respect to a practically zero background. On the other hand, open path fluorescence is usually much more difficult to implement and calibrate. Using open path absorption, an average concentration over a long distance can be measured with the assumption that for a given local concentration the absorption contribution is the same for any distance from the emitter/receiver. In the case of fluorescence, the local return signal depends on the overlap function between the field of emission and the field of view of the receiver. And the fluorescence return drops

off as the square of the distance from the receiver for a constant excitation power. But the excitation power drops off depending on extinction and absorption. It is difficult to take all this into account in a non-lidar approach. There usually is a calibration channel for the excitation power in a fluorescence lidar, such as the Raman from nitrogen in air. This is not available with a LED. Doing path integrated fluorescence would require careful receiver construction, calibration and some way of calibrating the effective local excitation power. Moreover, benzene fluorescence is partially quenched in air because of oxygen. It is not known by the authors if other variable air constituents quench the benzene fluorescence, CO₂ for example. Not having a retroreflector at one end of the open path is an interesting advantage. So although potentially more sensitive, it is much more complex. Work is nonetheless underway to see if fluorescence on a short distance from the emitter/receiver can be a reasonable option.

Preliminary tests were done using a spectroscopic lidar described elsewhere⁸. This is by no way a simple, low cost, low complexity system. It uses a frequency doubled pulsed tunable visible OPO (Solar LS Belarus, models LP603 & LG350), a large aperture (20 cm diameter) custom collection telescope, a grating spectrograph (Andor model Shamrock 163) and intensified charge coupled device (ICCD) UV camera (Andor iStar 734) capable of a few nanoseconds gating. The fluorescence is coupled to the spectrograph through a UV transmitting fiber bundle (hexagonal at the telescope focal plane and line at the spectrograph entrance) and optics to match the f-number of the incoming light to that of the spectrograph. A high pass (Razor Edge, Semrock) interference filter is placed in front of the fiber bundle to filter the laser light. A different filter is used for the different excitation wavelengths. Benzene fluorescence generated by absorption at 247.1, 252.9 and 258.9 nm was measured in both nitrogen and air. The benzene was in the same stainless steel cell as described previously. It was placed at ~10 m from the lidar. The average laser power was approximately 1 mW (220 to 220 μJ at 10 Hz in 6 to 9 ns pulses). The laser linewidth was ~0.03 nm. The benzene concentrations used were 1000 ppm in nitrogen (or 100 ppm-m) and 100 ppm in air (or 10 ppm-m), both at atmospheric pressure.

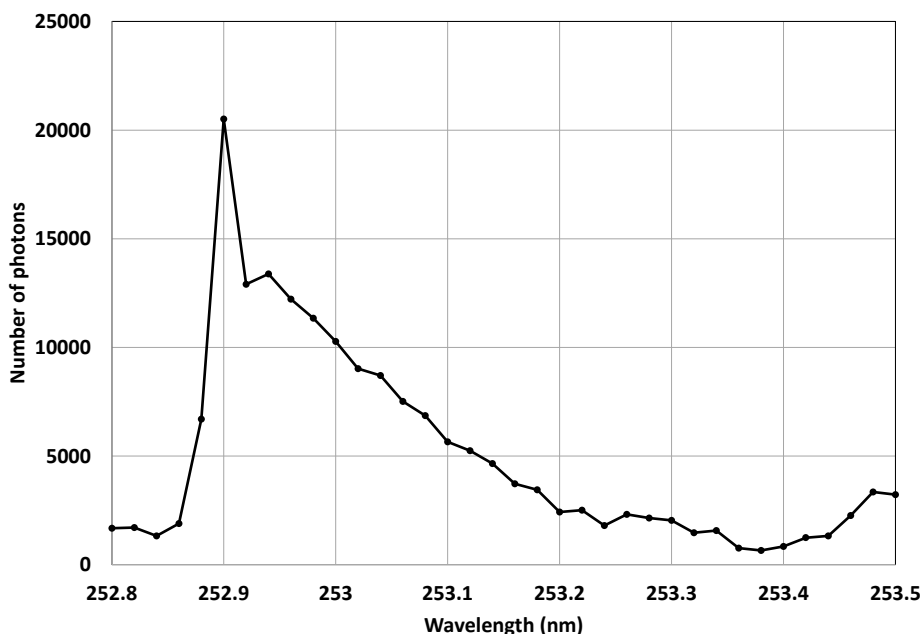


Figure 6. Integrated fluorescence between 265 and 300 nm with respect to laser excitation wavelength for 100 ppm of benzene in air at atmospheric pressure in a 10 cm cell at 10 m from the lidar.

With this experimental lidar, benzene fluorescence was easily measured. Figure 6 shows the fluorescence excitation spectrum (which mirrors the absorption spectrum). Fluorescence spectra are measured at each wavelength step with a spectral resolution of ~0.3 nm (not shown here) and then the signal is digitally integrated between 265 and 300 nm (in the solar blind region). The laser wavelength is scanned with 0.02 nm steps. Fluorescence intensity is not corrected for varying laser power (but laser power does not change significantly over less than a nanometer). Integrated fluorescence is not zero before the major benzene peak because of return from constituents in the air and fluorescence from the cell windows. The ICCD gate was 10 ns (~5 feet of laboratory air), shorter than the measured fluorescence lifetime in

nitrogen (~40 ns at 1/e). The signal is measured over 100 pulses (10 seconds). Fluorescence was much stronger in nitrogen than in air which indicates quenching in air. Lowering the pressure in the cell to just a few 10's of mbars, the fluorescence of benzene in air grew significantly. Our point is that measuring benzene in air at atmospheric pressure, using fluorescence generated by a LED, in an open path configuration is possible, especially if measured over 5 minutes. A detection limit cannot be given at this point. Although the LED has a much larger spectral bandwidth than the laser, the fluorescence excitation spectrum is relatively large (it follows the absorption spectrum). And fluorescence would be generated with both the 252.9 nm and 258.9 nm bands. It is thus expected that the LED could generate measurable fluorescence in an open path configuration.

6. CONCLUSION

While it is an interesting approach, the gas correlation, as reported here, in the deep UV, has important drawbacks. The stated goal was to develop a compact, low cost, field deployable benzene specific open path detector concept. This was achieved. But in order for this to work as expected, the LEDs need to be temperature stabilized to a high degree or filtered to the point where the gas correlation is not much of an advantage. The gas correlation spectrometer does not allow the signal processing possible with the UV-DOAS approach. Some of the drawbacks come from the use of two LEDs, one that is filtered by the gas correlation cell, and the other not. The baseline would be more stable if a single LED was used (see for example ⁹). The modulation would then need to be mechanical (a rotating chopper wheel for instance). Although an instrument with no moving parts is preferable, if the single LED plus mechanical chopper could give much better results, it is worth exploring. These preliminary results indicate that it would be possible to reach the ppb concentration level for 300 m open path lengths.

The fact remains that the deep UV LEDs are a promising optical source for open path optical absorption work in the deep UV. The fact also remains that if it is not stability on the order of 100 ppb-m that is the goal, the gas correlation approach with LEDs retains its advantages. And work is ongoing to reduce the baseline drift and to test a LED based fluorescence approach.

REFERENCES

- [1] Thoma, E., Thompson, E., Dewees, J., Deshmukh, P., Wisniewski, T., McEwan, S., Sosna, D., Weiss, H., Gross-Davis, C., Schmidt, H., "Testing of Cerex Open-Path Ultraviolet Differential Optical Absorption Spectroscopy Systems for Fenceline Monitoring Applications," Extended abstract presented at Air & Waste Management Association Air Quality Measurement Methods and Technology Conference, Chapel Hill, NC, March 15 - 17, 2016.
- [2] Kern, C., Trick, S., Rippel, B., Platt, U., "Applicability of light-emitting diodes as light sources for active differential optical absorption," *Applied Optics* 45(9), 2077-2088 (2006).
- [3] Hirayama, H., Fujikawa, S., Noguchi, N., Norimatsu, J., Takano, T., Tsubaki, K., Kamata, N., "222–282 nm AlGaIn and InAlGaIn-based deep-UV LEDs fabricated on high-quality AlN on sapphire," *Physica Status Solidi a*, 206(6), 1176-1182 (2009).
- [4] Fally, S., Carleer, M., and Vandaele, A. C., "UV Fourier transform absorption cross sections of benzene, toluene, meta-, ortho-, and para-xylene," *Journal of Quantitative Spectroscopy and Radiative Transfer*, 110(9-10), 766-782 (2009).
- [5] Kebedian, P.L., Annen, K.D., Berkoff, T.A., Freedman, A., "Nitrogen dioxide sensing using a novel gas correlation detector," *Meas. Sci. Technol.* 11, 499-503 (2000).
- [6] Dakin, J.P., Gunning, M.J., Chambers, P. and Xin, Z.J., "Detection of gases by correlation spectroscopy," (In special issue: Proceedings of the 6th European Conference on Optical Chemical Sensors and Biosensors EUROPT(R)ODE VI) *Sensors and Actuators B: Chemical* 90(1-3), 124-131 (2003).
- [7] Vulcanescu, L., Galais, A., Dorlhene, P., "Mesure en continu du benzène par voie optique (InC-Interferometric Correlation) Application aux rejets automobiles," *Pollution Atmosphérique* 169, 111-125 (2001).
- [8] Babin, F., Gravel, J.-F., Allard, M., "Airborne pipeline leak detection: UV or IR?," *Proc. SPIE* 9824, Chemical, Biological, Radiological, Nuclear, and Explosives (CBRNE) Sensing XVII, 982417 (May 12, 2016).
- [9] Lou, X.T., Somesfalean, G., Zhang, Z.G., Svanberg, S., "Sulfur dioxide measurements using an ultraviolet light-emitting diode in combination with gas correlation techniques," *Appl. Phys. B* 94, 699-704 (2009).